Actuator-Line Model in a Lattice Boltzmann Framework for Wind Turbine Simulations

S. Rullaud, F. Blondel, M. Cathelain

Actuator-Line Model in a Lattice Boltzmann Framework for Wind Turbine Simulations

IOP Conf. Series: Journal of Physics: Conf. Series **1037** (2018) 022023 doi:10.1088/1742-6596/1037/2/022023

Actuator-Line Model in a Lattice Boltzmann Framework for Wind Turbine Simulations

S. Rullaud, F. Blondel, M. Cathelain

IFP Energies nouvelles, 1-4 avenue du Bois Préau, 92852 Rueil-Malmaison, France

E-mail: `frederic.blondel@ifpen.fr`

Abstract.

This paper presents the development of a solver based on a Lattice Boltzmann Method (LBM) to perform reliable wind turbine simulations: *LaBoheMe*. LBM offers an interesting framework with low dissipation and high performance computing compared to usual Computational Fluid Dynamics (CFD) solvers based on Navier-Stokes equations. In order to take wind turbines into account in the LBM solver, *LaBoheMe* is enhanced by the addition of local force terms representing the influence of the wind turbines on the flow. These forces are computed using an Actuator-Line Model (ALM). The present solver is a 2D LBM/ALM solver allowing the simulation of "slices" of a Vertical Axis Wind Turbine (VAWT).

The Lattice Boltzmann and the Actuator Line methods are described and the coupling adopted in this work is detailed. Validation cases for pure LBM (Backward Facing Step, BFS) and coupled LBM/ALM are performed. The LBM/ALM coupling is validated against experimental data and compared with a vortex method and a large eddy simulation of the wake. Both blade forces and wake velocities are considered.

1. Introduction

Nowadays, most of the CFD solvers used for wind turbine simulations are based on Navier-Stokes equations. In this framework, the finite-volume discretization method prevails, although it can be diffusive to some extent. As an alternative, vortex methods, such as the ones currently used at IFPEN (see Blondel et al., [7] and Blondel et al., [5]), are getting more interest since their diffusivity is limited. However, the vortex methods used at IFPEN are limited to inviscid flows or flows with artificial viscosity from empirical laws. Still, viscosity can be introduced in such methods (see Chatelain et al., [8] and Pinon et al., [24]), but it increases both computational time and complexity. In the present work, a modern approach is adopted: the Lattice Boltzmann Method. LBM does not consist in approximating the Navier-Stokes equations, but instead uses the Boltzmann equation to describe the physics at a mesoscopic level. At such a scale, the fluid is represented by particles, and their motions are defined statistically. This method captures exact transport phenomena and provides high parallelisation capabilities, as most of the operations occur at the node level.

Although LBM is increasingly used in many CFD applications, such as flows in porous media (see Kutscher et al., [16]), multiphase flows (see Zheng et al., [29]) or aero-acoustics (see Marié, [18]), it is not a common solution for wind turbine simulations.

Recently, Deiterding et al. [10] and Pérot et al. [23] used an LBM solver to compute the flow around wind turbine rotors and farms, using immersed boundaries to take the wind turbines into account. Another way of modelling wind turbines is to use the Actuator Line Method (ALM) (see Sørensen and Shen, [27]), based on the Blade Element theory and the description of the airfoil polars, rather than a full representation of wind turbine blades. Such an approach strongly reduces the computational cost. The ALM interacts with the LBM to get the flow field at each node in order to compute the forces acting on the wind turbine blades. Afterward, the resulting forces are applied to the flow through forcing terms added to the conventional LBM model.

In order to validate the coupling, two test cases are considered: the "Strickland VAWT" (see Strickland et al., [28] and Nguyen [20]) for blade forces and the "IMST VAWT" (see Fraunié et al., [13]) for wake velocities. Results are compared to experiments, a vortex method (see Blondel and Cathelain, [6]) and an LES simulation (see Porté-Agel et al., [26]). The current code, namely *LaBoheMe*, is currently limited to a 2D model for vertical axis wind turbines. To the author's best knowledge, it is the first time a coupling of the LBM and ALM methods is implemented.

2. LBM and ALM methods

2.1. Lattice Boltzmann method

Within the LBM framework, the Boltzmann equation is solved on a discrete lattice. Even though LBM is not based on the Navier-Stokes equations, these equations can be recovered from the discrete Boltzmann equations (see D'Humières et al., [25]). The fluid is composed of particles. Motions of the particles are defined as the probability particles have to travel in a direction. A distribution function f is defined. This function depends on the position x, the velocity c and the time t, and its evolution follows the Boltzmann equation:

$$\frac{\partial f}{\partial t} + c\frac{\partial f}{\partial x} + \frac{F}{m}\frac{\partial f}{\partial c} = \left(\frac{\partial f}{\partial t}\right)_{col}, \tag{1}$$

where F is an external body force acting on the flow (e.g. related to the presence of the wind turbines in our case), and m the particle's mass. This equation is divided into three different parts:

- $\frac{\partial f}{\partial t} + c\frac{\partial f}{\partial x}$ represents the advection (or *streaming*) of the particles.
- $\left(\frac{\partial f}{\partial t}\right)_{col}$ is the collision term.
- $\frac{F}{m}\frac{\partial f}{\partial c}$ is a source term.

The method consists in applying this equation on a regular Cartesian lattice (although this is not a strict condition, see Peng et al., [22]). Particles are located on the nodes of the lattice and have several permitted streaming directions. Many LBM models have been studied in the literature, each model corresponding to a particular dimension "D" and set of directions "Q". The most common models are the $D2Q9$ model illustrated in Figure 1 and the $D3Q19$ model, respectively 2D with 9 streaming directions $\vec{e_i}$ and 3D with 19 streaming directions. Equation (1) is discretized and is called Lattice Boltzmann Equation. During the *streaming* step, the distribution functions f_i are propagated to the neighboring nodes of the lattice in the permitted i directions following Equation (2):

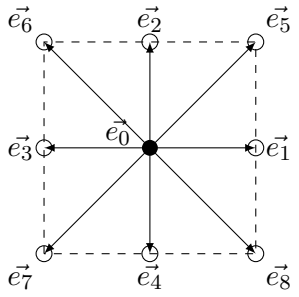

Figure 1. Geometry of the D2Q9 model

$$f_i\left(\vec{x}+\vec{e_i}\Delta t, t+\Delta t\right) = f_i\left(\vec{x}, t\right), \tag{2}$$

Δt being the time step of the simulation. The density and momentum are deduced from the distribution functions f_i with the following expressions:

$$\rho = \sum f_i, \tag{3}$$

$$j_\alpha = \rho u_\alpha = \sum \overrightarrow{e_{\alpha i}} f_i. \tag{4}$$

The *collision step* can be defined by different operators. The simplest one is the BGK collision operator named from Bhatnagar, Gross and Krook (see [4]). This step consists in considering the collision as a relaxation of distribution functions toward an equilibrium state with a relaxation time τ. Another collision operator is the Multiple Relaxation Time (MRT) operator (see dHumières et al., [11]): this operator is more complex, each quantity (i.e. density, momentum, energy...) having its own relaxation time as expressed in Equation (5). This description is more realistic, since each quantity does not need the same time to reach its equilibrium state f_i^{eq}. Lallemand and Luo demonstrated the superiority of the MRT above the BGK operator [17]. The MRT operator is more stable and requires fewer hypotheses than BGK operator.

A diagonal matrix S_D is introduced in Equation (5) to take into account the various relaxation times. Values from the Palabos documentation [2] are used, but the relaxation times related to the LBM viscosity and the LBM velocity remain unknown. Following Palabos recommendations, the LBM velocity u_{LBM} is set to 0.01. All of the remaining relaxation times are then deduced from the LBM velocity.

$$f_{i,collision}\left(\vec{x}+\vec{e_i}\Delta t, t+\Delta t\right) = f_i\left(\vec{x}+\vec{e_i}\Delta t, t+\Delta t\right) - S_D\left[f_i\left(\vec{x}, t\right) - f_i^{eq}\left(\vec{x}, t\right)\right]. \tag{5}$$

The distribution functions at equilibrium are related to the momentum through a transformation matrix M:

$$f^{eq} = M^{-1} m^{eq}, \tag{6}$$

with:

$$M = \begin{pmatrix} 1 & 1 & 1 & 1 & 1 & 1 & 1 & 1 & 1 \\ -4 & -1 & -1 & -1 & -1 & 2 & 2 & 2 & 2 \\ 4 & -2 & -2 & -2 & -2 & 1 & 1 & 1 & 1 \\ 0 & 1 & 0 & -1 & 0 & 1 & -1 & -1 & 1 \\ 0 & -2 & 0 & 2 & 0 & 1 & -1 & -1 & 1 \\ 0 & 0 & 1 & 0 & -1 & 1 & 1 & -1 & -1 \\ 0 & 0 & -2 & 0 & 2 & 1 & 1 & -1 & -1 \\ 0 & 1 & -1 & 1 & -1 & 0 & 0 & 0 & 0 \\ 0 & 0 & 0 & 0 & 0 & 1 & -1 & -1 & -1 \end{pmatrix}. \tag{7}$$

Some of the macroscopic quantities are invariant through collision due to the mass and momentum conservation, thus $\rho = \rho_{eq}$ and $j_\alpha = j_{\alpha eq}$. For the other macroscopic quantities, equilibrium values are derived from the density ρ and the momentums j_α as follows:

$$m^{eq} = \begin{pmatrix} \rho \\ e \\ \epsilon \\ j_x \\ q_x \\ j_z \\ q_z \\ \sigma_{xx} \\ \sigma_{xz} \end{pmatrix}^{eq} = \begin{pmatrix} \rho \\ -2\rho + 3\left(u_x^2 + u_z^2\right)\rho^2 \\ \rho - 3\left(u_x^2 + u_z^2\right)\rho^2 \\ u_x\rho \\ -u_x\rho \\ u_z\rho \\ -u_z\rho \\ \left(u_x^2 - u_z^2\right)\rho^2 \\ u_x u_z \rho^2 \end{pmatrix}, \tag{8}$$

where ρ is the local density, e is the energy, ϵ is the energy squared, j_x and j_z are the momentums, q_x and q_z are the fluxes and σ_{xx} and σ_{xz} are stresses.

The last step is the addition of external forces induced by the wind turbine blades. Several methods exist (see Huang et al., [14]). The chosen method is the so-called "exact difference method" suggested by Kupershtokh et al. [15]. It is directly derived from the Boltzmann equation. It consists in adding a source term S_i to the streaming and collision equations (9).

$$S_i = f_i^{eq}\left(\rho, \vec{u}^{eq} + \Delta\vec{u}\right) - f_i^{eq}\left(\rho, \vec{u}^{eq}\right) : \tag{9}$$

with

$$\Delta\vec{u} = \frac{\vec{F}\Delta t}{\rho}. \tag{10}$$

At each step, the LBM provides distribution functions on the full domain. Macroscopic quantities associated with each node are then derived.

This summary of the Lattice Boltzmann method highlights the simplicity of the operations implemented in the method: only linear combinations are needed. In addition, most of the operations on the nodes are independent from their neighbors (at least during the collision phase), thus, parallelisation can be easily implemented (see OpenLB documentation, [1]).

2.2. Actuator line method

In the previous section, the modelling of the flow has been described. This section introduces the wind turbine inside the Lattice Boltzmann model: the wind turbine blades are modeled as actuator lines. At each step, the LBM solver computes the density and velocity on the lattice domain. The wind turbine blades rotate inside the domain and an averaged density-velocity description around the line is computed. The forces occurring on the blades (i.e. drag D and lift L) are derived from the airfoil polars and the attack angle α as shown in Figure 2.

The relative velocity $\vec{u}_{rel}$ is defined as:

$$\vec{u}_{rel} = \vec{u}_{wind} - \vec{u}_{displacement}, \tag{11}$$

and, the focus being on VAWT, the attack of angle varies during the rotation of the blades. It is computed using the flow velocities projected in the local blade element reference frame:

$$\alpha = atan2\left(\frac{u_T^{rel}}{u_N^{rel}}\right), \tag{12}$$

u_N^{rel} being the relative velocity seen by the profile in the normal direction with respect to its chord line, and u_T^{rel} the tangential counter-part.

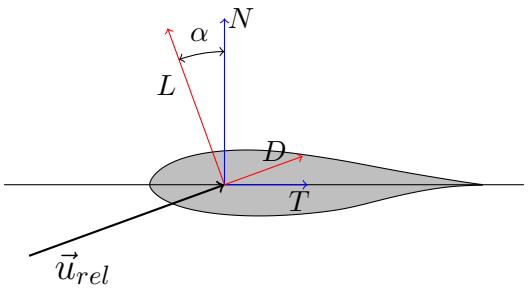

Figure 2. Angle of attack and forces acting on an airfoil

In addition, a stall model is implemented in the force calculation. The chosen one is the Øye stall model [21] modified by Blondel et al. [7]. It represents the time lag of the separation point displacement on the suction side of the airfoil.

The force are located on a 2D line, thus a Gaussian spreading function is implemented in order to take into account a volumic force:

$$\vec{f}_\epsilon(d) = \frac{1}{\epsilon^2 \pi} \exp\left(-(d/\epsilon)^2\right) \vec{f}. \tag{13}$$

This Gaussian repartition is a 2D-isotropic distribution, based on a spreading length ϵ that is set proportional to the chord length of the airfoil. Other definitions exist to have a better representation of the physics, such as a non-isotropic projection that mimics the force distribution around an airfoil (see Churchfield et al., [9]).

As an illustration, a VAWT and its numerical counter-part are given in Figures 3 and 4.

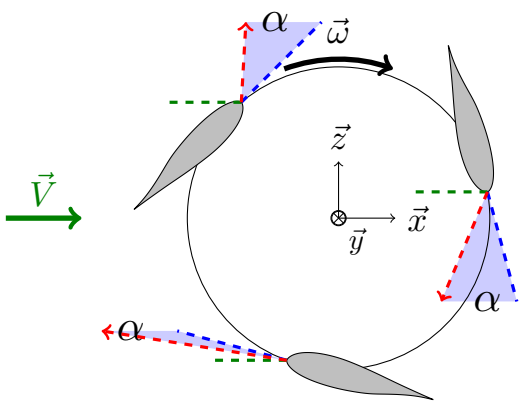

Figure 3. Diagram of a VAWT

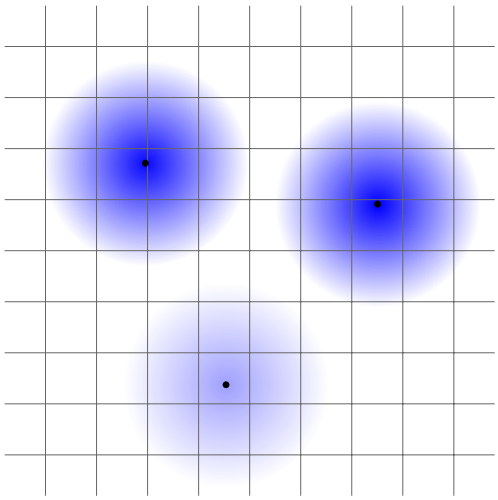

Figure 4. Vertical axis wind turbine described with ALM on a LBM lattice

3. Validation

3.1. Pure Lattice Boltmann method validation, Backward Facing Step (BFS)

The focus of this work being the modelling of a VAWT, a 2D model is sufficient in a first approach (tip vortices are excluded from the simulations). The $D2Q9$ MRT scheme illustrated in Figure 1 is used. The inlet/outlet boundary conditions suggested by Zou and He [30] are implemented and a bounce-back scheme is used to represent the no-slip conditions at the walls.

Figure 5. Representation of the Backward Facing Step computational domain

The in-house LBM solver is tested through a classical benchmark called the backward facing step (BFS), illustrated in Figure 5. The flow comes from the left of the domain. The Laser-Doppler experimental measurements of Armaly et al. ([3]) are used to compare with our simulations. Two different Reynolds numbers are considered: $\mathcal{R}e = 100$ and $\mathcal{R}e = 389$. This Reynolds number is based on the hydraulic diameter of the inlet channel and the two-thirds of the maximum inlet velocity.

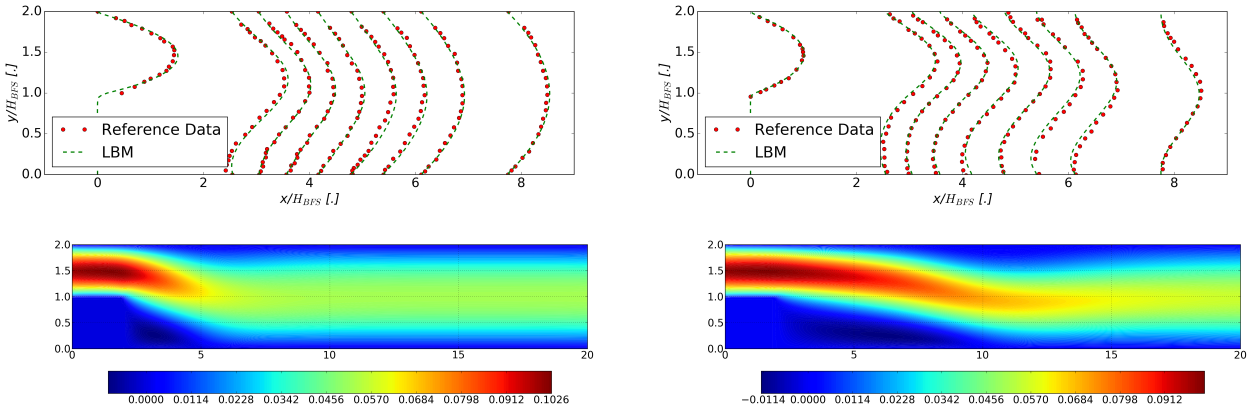

Figure 6. Backward Facing Step validation, $Re = 100$ (right), $Re = 389$ (left)

The results obtained through the LBM model in Figure 6 show very good agreement with the experimental data for both regimes. As expected, a circulation area is fed by the upstream flow and occurs downstream the step. The length of this circulation zone depends on the Reynolds number. Further downstream, the influence of the step disappears because of the fluid viscosity, and the outgoing flow tends towards the expected Poiseuille profile.

This benchmark validates the treatment of the boundaries (inlet, outlet, and walls), and the LBM implementation.

3.2. Coupled LBM/ALM, Vertical Axis Wind Turbine
The LBM flow solver being validated, VAWT can now be considered. The validation is based on two complementary tests: blade forces prediction on one hand and wake velocity prediction on the other hand.

3.2.1. "Strickland VAWT" - Blade forces The first test concerns the comparison of the predicted blade forces to the measured ones. As a reminder, the normal and tangential forces on the blades are computed by the solver using the macroscopic quantities (density and velocities) derived from the LBM distribution functions. Forces depend on the angle of attack of the profile, the airfoil polar and the stall model. In the upwind part of the VAWT (between azimuth 0 and azimuth 180^o), the incoming flow is free from any disturbance from the rotor except pressure effects. At the downwind position, the incoming flow is modified by the wake generated by the blades at the upwind position.

The validation of the force calculation is based on the "*Strickland VAWT*" test case. Experiments led by Nguyen and Strickland et al. [20] and [28] on this rotor are used as a reference, in complement with 2D vortex simulations with no stall and no boundaries (see Blondel and Cathelain, [6]). Experiments were performed in a water tow tank with a chord based Reynolds number of 40000. The 2-blade VAWT is dragged through the tank at different tip speed ratios (TSR). The dimensionless values of the normal and tangent forces are extracted at the blades as follows:

$$F^*_{n,t} = C_{n,t} \times \frac{U_{rel}}{U_\infty}, \tag{14}$$

with

$$C_{n,t} = \frac{F_{n,t}}{\frac{1}{2}\rho {U_{rel}}^2 chord}. \tag{15}$$

$F^*_{n,t}$ are respectively the dimensionless normal and tangential forces while $C_{n,t}$ are the normal and tangential forces coefficients. In addition, U_{rel} is the relative velocity and U_∞ is the infinite velocity. Four complete rotor revolutions are performed, to be consistent with the measurements. 1500 lattices are used in the axial direction. The results obtained at $TSR = 2.5, 5.0$ are presented in Figure 7.

Different phenomena are observed. Upwind, while the azimuth angle α is increasing, the angle of attack and then both lift and drag coefficients increase. It leads to an increase of both normal and tangential forces. α finally decreases after a peak around 90^o of azimuth angle. Downwind, the angle of attack becomes negative, thus, the lift decreases but the drag increases. In addition to this phenomenon, the incoming velocity is reduced due to disturbances (wakes) created upstream, which results in lower amplitude of the angle of attack in the downstream region compared to the upstream ones. It explains the lower amplitude of the normal and tangential forces.

All simulations present this characteristic, there is a match between the forces calculated in both models and the experiment. However, some discrepancies appear, for instance the vortex method does not show the bump around 270^o. Few aerodynamic models for VAWTs, such as the Actuator Cylinder flow model, predict this bump (see Ferreira et al., [12]). In addition, the stall model is the only one to reproduce the high increase of tangential forces at downwind positions. As a summary, the *LaBoheMe* solver with the Øye stall model has a good representation of the physics and compares well with the experimental data.

The coupling of a LBM solver with an actuator line model of turbine is encouraging.

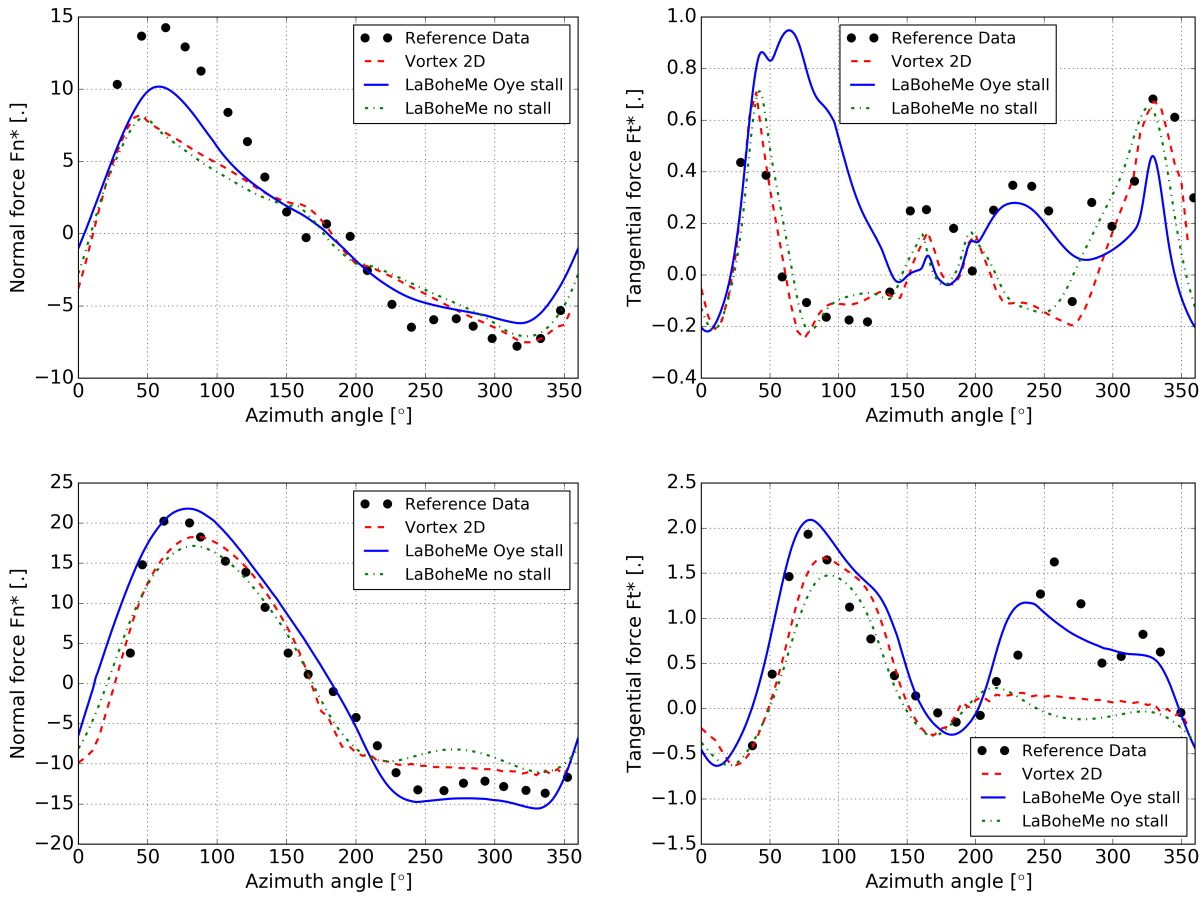

Figure 7. Strickland case, normal (right) and tangent (left) forces for $TSR = 2.5$ (up) and $TSR = 5.0$ (down)

3.2.2. "IMST VAWT" - Wake velocities The second test compares measured velocities in the wake to the simulated ones. The velocity in the channel downstream the turbine is measured using a Particle Image Velocimetry (PIV) system.

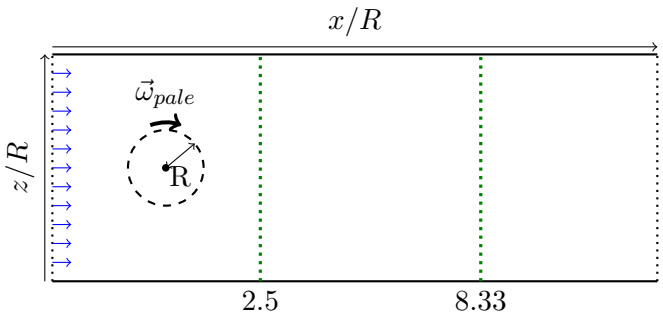

Figure 8. IMST section scheme

The benchmark used for the wake validation is the "IMST VAWT" [13]. The experiment occurs in a vertical channel with running water at $\mathcal{R}e = 10000$ and static VAWT. The wake velocity is measured at several sections positioned behind the rotor as shown in Figure 8. In this case, wake recovery due to the viscosity must be observed while the section is getting farther downstream from the rotor. This phenomenon is missing from the Vortex model that is why another reference is chosen. The LES simulations of Shamsoddin and Porté-Agel presented in [26] are elected for being this reference. Shamsoddin and Porté-Agel combined an LES with an ALM model for VAWT simulation which was tested on the "IMST VAWT" case.

The results presented here are the comparison of the experiments conducted at the IMST with the LES model and the *LaBoheMe* results of a 2-blade Darrieus turbine at TSR= 3.85. 40 full rotor revolutions are performed and 1500 lattices are used in the axial direction. The wake profiles at sections $x/R = 2.50$ and $x/R = 8.33$, where R is the rotor radius, are shown in Figure 9.

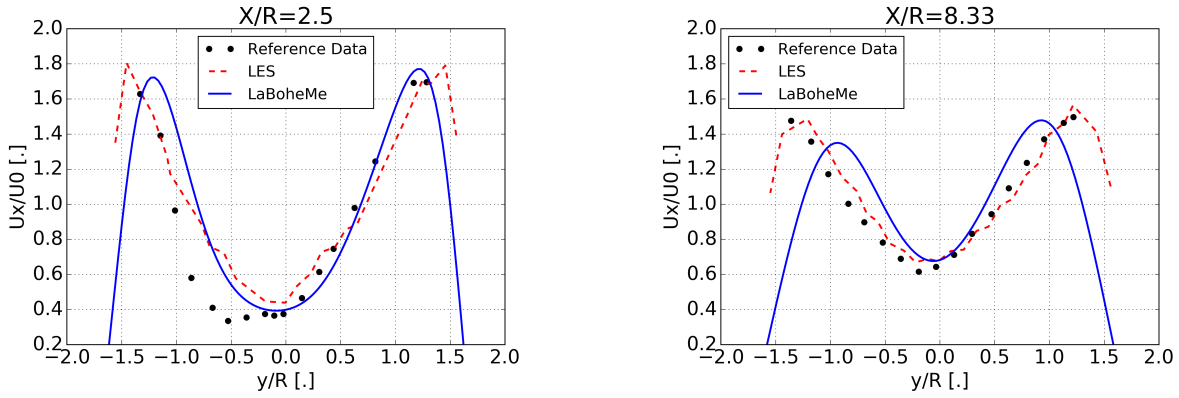

Figure 9. IMST case, Wake velocities at sections $X/R = 2.50$ (right) and $X/R = 8.33$ (left)

The IMST case highlights the flow propagated downstream the VAWT. The velocity has been modified by the rotor. Close to the wall, a blocking effect is created at $\mid y \mid > R$, it increases the flow velocity around the turbine. On the contrary, for $\mid y \mid < R$, the velocity decreases due to the wake creation. At a section farther from the rotor, a dissipation phenomenon due to the viscosity reduces the amplitude of the wake: the velocity for $\mid y \mid > R$ decreases and for $\mid y \mid < R$ is increases. Results show good agreement between the reference data, the LES and the *LaBoheMe* solver. Even though the LES gives closer results to the reference data than *LaBoheMe* does, *LaBoheMe* needs fewer operations to deliver good results (see Marié et al., [19]).

4. Conclusion

This study has highlighted the interest of coupling Lattice Boltzmann and Actuator line methods. Indeed, *LaBoheMe* model shows suitable results compared to experiments, vortex and LES models. The addition of a stall model is even improving the results. The addition of an external force as a source term works well. These results are promising since the method does not have a turbulence model yet. The results presented in this paper are validating the coupling of the LBM and ALM. *LaBoheMe* is able to deliver accurate results with fewer operations than finite volume solvers. In the future, the impact of the spreading function used to incorporate forces will be tested and a turbulence model will be added to the Lattice Boltzmann model such as a Smagorinsky model. Furthermore, a complementary study is being led in order to create a 3D version of *LaBoheMe*. It will be adapted to horizontal axis wind turbines.

References

[1] Openlb website. `http://optilb.org/openlb/`. Accessed: 2017-03-06.
[2] Palabos website. `http://www.palabos.org/`. Accessed: 2017-03-06.
[3] B. Armaly, F. Durst, J. Pereira, and B. Schönung. Experimental and theoretical investigation of backward-facing step flow. *J. Fluid Mech.*, 127, 1983.
[4] P.L. Bhatnagar, E.P. Gross, and M. Krook. A model for collision processes in gases. i. small amplitude processes in charged and neutral one-component systems. *Phys. Rev.*, 94, 1954.
[5] F. Blondel, R. Boisard, M. Milekovic, G. Ferrer, C. Lienard, and D. Teixeira. Validation and comparison of aerodynamic modelling approaches for wind turbines. *J. Phys. Conf. Ser.*, 753(2):22–29, 2016.
[6] F. Blondel and M. Cathelain. Benchmarking activities (code to code comparison) on the rigid 1hs 3-bladed vawt. Technical report, 2017.
[7] F. Blondel, G. Ferrer, M. Cathelain, and D. Teixeira. Improving a bem yaw model based on newmexico experimental data and vortex cfd simulations. Congrés Français de Mécanique, 2017.
[8] P. Chatelain, M. Duponcheel, D. Caprace, Y. Marichal, and G. Winckelmans. Vortex particle-mesh simulations of vertical axis wind turbine flows: from the airfoil performance to the very far wake. *Wind Energ. Sci.*, 2:317–328, 2017.
[9] M. Churchfield, S. Schreck, L. Martínez-Tossas, C. Meneveau, and P. Spalart. An advanced actuator line method for wind energy applications and beyond. 2017.
[10] R. Deiterding and S. Wood. Predictive wind turbine simulation with an adaptative lattice boltzmann method for moving boundaries. *Journal of Physics: Conference Series*, 753, 2016.
[11] D. dHumières, I. Ginzburg, M. Krafczyk, P. Lallemand, and L.S. Luo. Multiple-relaxation-time lattice boltzmann models in 3d. *ICASE Report No. 2002-20*, 2002.
[12] C. Ferreira, H. Madsen, M. Barone, B. Roscher, P. Deglaire, and I. Arduin. Comparison of aerodynamic models for vertical axis wind turbines. *Journal of Physics: Conference Series*, 524, 214.
[13] P. Fraunie, C. Beguier, I. Paraschivoiu, and G. Brochier. Water channel experiments of dynamic stall on darrieus wind turbine blades. *J. Prop. Power*, 2:445–449, 1986.
[14] H. Huang, M. Krafczyk, and X. Luo. Forcing term in single-phase and shan-chen-type multiphase lattice boltzmann models. *Phys.Rev. E*, 2011.
[15] A. Kupershtokh, D. Medvedev, and D. Karpov. On equations of state in a lattice boltzmann method. *Computers & Mathematics with Applications*, 58:965–974, 2009.
[16] K. Kutscher, M. Geier, and M. Krafczyk. Multiscale simulation of turbulent flow interacting with porous media based on a massively parallel implementation of the cumulant lattice boltzmann method. *Computers and Fluids*, 2018.
[17] P. Lallemand and L. Luo. Theory of the lattice boltzmann method: dispersion, dissipation, isotropy, galilean invariance, and stability. *Phys.Rev. E*, 61, 2000.
[18] S. Marié. *Etude de la méthode Boltzmann sur Réseau pour les simulations en aroacoustique*. PhD thesis, Université Pierre et Marie Curie, 2008.
[19] S. Marié, D. Ricot, and P. Sagaut. Comparison between lattice boltzmann method and navierstokes high order schemes for computational aeroacoustics. *J. of Comp. Phys.*, 228:1056–1070, 2009.
[20] T. Nguyen. *A Vortex Model of the Darrieus Turbine*. PhD thesis, Texas Tech University, 1978.
[21] S. Øye. Dynamic stall simulated as time lag of separation. Technical report, 1991.
[22] G. Peng, H. Xi, C. Duncan, and S.-H. Chou. Lattice boltzmann method on irregular meshes. *Phys. Rev.*, 58, 1998.
[23] F. Pérot, M. Kim, M. Meskine, and D. Freed. Nrel wind turbine aerodynamics validation and noise predictions using a lattice boltzmann method. 2012.
[24] G. Pinon, P. Mycek, G. Germain, and E. Rivoalen. Numerical simulation of the wake of marine current turbines with a particle method. *Renewable Energy*, 46:111–126, 2012.
[25] Y. Qian, D. D'Humières, and P. Lallemand. Lattice bgk models for navier-stokes equation. *EPL (Europhysics Letters)*, 17:479–484, 1992.
[26] Sina Shamsoddin and Fernando Porté-Agel. Large eddy simulation of vertical axis wind turbine wakes. volume 7, pages 890–912. MDPI, 2014.
[27] J. Sørensen and W. Shen. Numerical modeling of wind turbine wakes. *Journal of Fluids Engineering*, 124:393–399, 2002.
[28] J. Strickland, T. Smith, and K. Sun. Vortex model of the darrieus turbine: an analytical and experimental study. final report. Technical report, 1981.
[29] H.W. Zheng, C. Shu, and Y.T. Chew. A lattice boltzmann model for multiphase flows with large density ratio. *J. of Comp. Physics*, 218, 2006.
[30] Q. Zou and X. He. On pressure and velocity boundary conditions for the lattice boltzmann bgk model. *Phys. Fluids*, 9:1591–1598, 1997.